Biology of Reproduction, 2020, 102(1), 233–247
doi:10.1093/biolre/ioz154
Research Article
Advance Access Publication Date: 3 September 2019

OXFORD

Research Article

COP9 signalosome complex subunit 5, an IFT20 binding partner, is essential to maintain male germ cell survival and acrosome biogenesis†

Qian Huang[1,2,‡], Hong Liu[1,3,‡], Jing Zeng[1,2,‡], Wei Li[2], Shiyang Zhang[1,2], Ling Zhang[1], Shizhen Song[1], Ting Zhou[1,2], Miriam Sutovsky[4], Peter Sutovsky[4], Ruggero Pardi[5], Rex A Hess[6] and Zhibing Zhang[2,7,*]

[1]Department of Occupational and Environmental Medicine, School of Public Health, Wuhan University of Science and Technology, Wuhan, Hubei, China, [2]Department of Physiology, Wayne State University, Detroit, Michigan, USA, [3]Institute of Reproductive Health, Center for Reproductive Medicine, Tongji Medical College, Huazhong University of Science and Technology, Wuhan, Hubei, China, [4]Division of Animal Sciences, College of Food, Agriculture and Natural Resources, and Department of Obstetrics, Gynecology and Women's Health, School of Medicine, University of Missouri, Columbia, Missouri, USA, [5]School of Medicine and Scientific Institute, San Raffaele University, Milan, Italy, [6]Comparative Biosciences, College of Veterinary Medicine, University of Illinois, Urbana, Illinois, USA, and [7]Department of Obstetrics/Gynecology, Wayne State University, Detroit, Michigan, USA

***Correspondence:** Department of Physiology, Department of Obstetrics/Gynecology, Wayne State University, 275 E Hancock Street, Detroit, Michigan 48201, USA. Tel: 313-5770442; E-mail: gn6075@wayne.edu

†**Grant Support:** This research was supported by NIH grant HD076257, HD090306 and Start up fund of Wayne State University and Wayne State University Research Fund (to ZZ), National Natural Science Foundation of China (81671514, 81571428, 81502792, 81300536, and 81172462), Excellent Youth Science Foundation (2018CFA040) and Youth Foundation of Hubei Province (2018CFB114), the China Scholarship Council Fund (201808420128), and Special Fund of Wuhan University of Science and Technology for Master Student's short-term studying abroad. Research in Sutovsky laboratory was funded by the National Institute of Food and Agriculture (NIFA), U.S. Department of Agriculture (USDA) grant number 2015-67015-23231 (PS), and seed funding from the Food for the 21st Century Program of the University of Missouri (PS).
‡These authors contributed equally to this study.

Received 16 February 2019; Revised 10 June 2019; Accepted 31 July 2019

Abstract

Intraflagellar transport protein 20 (IFT20) is essential for spermatogenesis in mice. We discovered that COPS5 was a major binding partner of IFT20. COPS5 is the fifth component of the constitutive photomorphogenic-9 signalosome (COP9), which is involved in protein ubiquitination and degradation. COPS5 is highly abundant in mouse testis. Mice deficiency in COPS5 specifically in male germ cells showed dramatically reduced sperm numbers and were infertile. Testis weight was about one third compared to control adult mice, and germ cells underwent significant apoptosis at a premeiotic stage. Testicular poly (ADP-ribose) polymerase-1, a protein that helps cells to maintain viability, was dramatically decreased, and Caspase-3, a critical executioner of apoptosis, was increased in the mutant mice. Expression level of FANK1, a known COPS5 binding partner, and a key germ cell apoptosis regulator was also reduced. An acrosome marker, lectin PNA, was nearly absent in the few surviving spermatids, and expression level of sperm acrosome associated 1, another acrosomal component was significantly reduced. IFT20 expression level was significantly reduced in the *Cops5* knockout mice, and it was no longer present in the acrosome, but remained in the Golgi apparatus of spermatocytes. In the conditional *Ift20* mutant

mice, COPS5 localization and testicular expression levels were not changed. COP9 has been shown to be involved in multiple signal pathways, particularly functioning as a co-factor for protein ubiquitination. COPS5 is believed to maintain normal spermatogenesis through multiple mechanisms, including maintaining male germ cell survival and acrosome biogenesis, possibly by modulating protein ubiquitination.

Summary sentence

COPS5 is essential for mouse spermatogenesis and particularly in maintaining male germ cell survival and acrosome biogenesis.

Key words: COP9 signalosome complex subunit 5, apoptosis, acrosome, spermatogenesis, male fertility

Introduction

COPS5 was initially identified as c-Jun activation domain-binding protein-1 (Jab1) [1], a c-Jun coactivator, and subsequently discovered to be the fifth component of the constitutive photomorphogenic-9 signalosome (COP9, CSN), which phosphorylates target proteins, leading to their ubiquitination and degradation by the 26S proteasome [2]. Therefore, COPS5 is also known as Jab1 and CSN5. COPS5 is a receptor within the COP9 signalosome and binds substrate proteins [3]. COP9, first identified in the plant, *Arabdopsis*, in 1992, was a multisubunit complex involved in signal transduction of photomorphogenesis [4]. Mammalian COP9 homolog was discovered in 1998, and purified mammalian COP9 complex contains eight subunits, named as S1–S8 according to its size on sodium dodecyl sulphate–polyacrylamide gel electrophoresis (SDS-PAGE) [5]. The COP9 complex is highly conserved among most multicellular eukaryotes, and nomenclature of the complex and its subunits was unified to avoid repeated nomenclature in different organisms, namely "the COP9 signalosome complex" [6]. COP9 signalosome complex plays multiple functions, including neddylation and ubiquitination [7, 8]; cell cycle control [9, 10]; apoptosis, especially for COPS5 through different pathways [11, 12]; cell proliferation, protein phosphorylation and signal transduction [13, 14]; DNA damage response; and tumorigenesis [15]. Among the subunits of the COP9, COPS5 receives more attention due to its unique characteristics, which include the following: (1) isopeptidase activity [16]; (2) functioning either as a subunit of the complex or as a single unit outside the complex [17, 18]; and (3) being the most conserved protein among the eight subunits [19].

COPS5 encodes a protein with a molecular mass of 38 kDa. It contains a c-Jun–binding domain that provides the catalytic center to the complex for the CSN isopeptidase activity [20–22], an Mpr1-Pad1-N-terminal domain that is responsible for regulating the cullin deneddylation process by activating the CRL Cullin-RING family of ubiquitin ligase activity [23–25], a nuclear export signal domain, and a p27-binding domain (PBD) at the C-terminal end. Through the binding of P27 to PBD, COPS5 carries p27 protein out of the cell nucleus [26].

Being a pivotal CSN subunit, COPS5 takes part in crucial biological activities of the CSN complex, mainly in the nucleus. However, the nuclear accumulation of COPS5 seems to be dependent on other CSN components [27]. A large portion of COPS5 was discovered in free form in both cytoplasm and nucleus. Therefore, a striking feature of COPS5 is its reported interaction with a wide range of proteins and its modulation of their activities and stability, suggesting a broad range of biological activities for the protein, particularly in tumorigenesis [28]. COPS5 has been shown to functionally interact with several tumor-related genes, including *p27*, *p57*, *MDM2*, and *p53*, *PD-L1*, *NcoR*, *Bcl2*. As an oncogene, it is aberrantly overexpressed in various human cancers [29–31], presumably through regulation of gene amplification, miRNA, and other signaling pathways, including IL6-Stat3, HER2-AKT, TGF-β, Wnt, NF-κB, MIF-PI3K-AKT, and Bcr-Abl signals [32–34].

As a major component of COP9, COPS5 is engaged in functions of the complex, such as in cell proliferation and cell cycle progression, apoptosis, DNA damage response, reactive oxygen species regulation, hypoxia, and senescence [35–37]. Besides cancer, COPS5 has been associated with a number of other diseases including the following: chronic mountain sickness [38]; Vitiligo [39]; foam cell formation and atherosclerotic [40]; cardiac hypertrophy [41]; amyloid pathology in vivo [42]; chronic rhinosinusitis; and nasal polyposis [43]. COPS5 also associates with the core-glycosylated form of cystic fibrosis transmembrane conductance regulator (CFTR) to target misfolded CFTR to the degradative pathway [44]. Recent discoveries have identified it as an intracellular (negative) modulator of BMP signaling in chondrocytes and other cells [45], and it is also necessary for T-cell signaling [46].

The function of COPS5 was also studied in mouse models. When the gene was inactivated globally, homozygous mutant embryos died soon after implantation, suggesting a role in early embryonic development and growth potential [47]. A floxed *Cops5* mouse model was generated, and the function of the gene in specific cell type/tissues was investigated. COPS5 acts at distinct developmental stages to coordinate proliferation, survival, and positive selection of thymocytes [48]. It is an essential regulator of early embryonic limb development in vivo [49].

Even though the role of COPS5 in somatic systems, particularly in cancer was intensively studied, few studies have been conducted to investigate its function in reproduction. It has been shown that COPS5 might be associated with the pathophysiology of preeclampsia [50], and in ovary, COPS5 is involved in oocyte meiosis and follicle differentiation [51, 52]. A testis-specific transcription factor, FANK1 has been shown to be a COPS5-binding partner [53, 54]. Fank1-knockdown transgenic mice displayed reduced sperm number and increased apoptotic spermatocytes [55]. Our laboratory has investigated the role of intraflagellar transport (IFT) proteins in male fertility and the regulation of spermiogenesis [56–59]. IFT20, a component of the IFT-B complex and essential for spermatogenesis, was used as bait in a yeast two-hybrid screen, and COPS5 was identified to be a major binding partner. Therefore, we hypothesized that COPS5 would have a role in ciliogenesis and thus formation of the flagellum during spermatogenesis. We first examined its localization in male germ cells and found that the protein was present in cytoplasm of spermatocytes, the acrosome of round spermatids,

and the acrosome and manchette of elongating spermatids. To further investigate its function in male germ cells, we used germ cell-specific conditional inactivation of the gene and discovered that the germ cells underwent dramatic apoptosis during meiosis. In the conditional knockout mice, male germ cells developed to round spermatids but showed defects in acrosome biogenesis. This study demonstrates that COPS5 participates in at least two important functions in male germ cells, regulation of spermatocyte apoptosis, and acrosome biogenesis.

Materials and methods

Ethics statement

All animal research was approved by Virginia Commonwealth University Institutional Animal Care (Protocol number: AD1000167) and Wayne State University Institutional Animal Care with the Program Advisory Committee (Protocol number: 18-02-0534).

Direct yeast two-hybrid assay

To detect the interaction between mouse COPS5 and mouse IFT20, full-length mouse *Ift20* and *Cops5* cDNAs were amplified using the following primers: *Ift20* forward: 5'-GAATTCATGGCCAAGGACA TCTTGGGC-3'; *Ift20* reverse: 5'-GGATCCCTTTCTGAAAAATAA ATTGGTC-3'; and *Cops5* forward: 5'-GAATTCATGGCAGCTTCC GGGAGTGGTA TG-3'; *Cops5* reverse: 5'-GGATCCCTAAGCAAC GTTAATCTGATTAAA-3'. After the TA clone and sequencing, the two cDNAs were cloned into pGADT7 and pGBKT7. IFT20/pGADT7 and COPS5/pGBKT7 were cotransformed into the AH109 host strain using the Match-Maker two-hybrid system 3 (Clontech, Mountain View, CA, USA) according to the manufacturer's instructions. The plasmid pGADT7 containing 40 large T antigen and plasmid pGBKT7 containing p53 were cotransformed into AH109 as the positive controls. The AH109 transformants were streaked out in complete drop-out medium lacking tryptophan, leucine, and histidine to test for histidine prototrophy.

Generation of *Cops5* conditional knockout mice

Cops5$^{flox/flox}$ mice were generated previously by Dr. Ruggero Pardi, and *Stra8-iCre* mice were purchased from the Jackson Laboratory (Stock No: 008208). To conditionally knockout *Cops5* gene in mouse germ cells, 3- to 4-month-old *Cops5*$^{flox/flox}$ females were crossed with 3 to 4-month-old *Stra8-cre* males to obtain *Stra8-iCre; Cops5*$^{flox/+}$ mice. Then, 3- to 4-month-old *Stra8-iCre; Cops5*$^{flox/+}$ males were crossed back with *Cops5*$^{flox/flox}$ females again. The *Stra8-iCre; Cops5*$^{flox/flox}$ were considered to be the homozygous KO mice, and *Stra8-iCre; Cops5*$^{flox/+}$ mice were used as the controls. Genomic DNA was isolated to genotype the offspring. The following primers were used for genotyping: *Stra8-iCre* forward: 5′-GTGCAAGCTGAACAACAGGA-3′; *Stra8-iCre* reverse: 5′-AGGGACACAGCATTGGAGTC-3′, *Cops5* forward: 5′-GCCTGCATTACCGGTCGATGCAACGA-3′; *Cops5* reverse: 5′-GTGGCAGATGGCGCGGCA-3′.

Assessment of fertility and fecundity

Cops5 KO and control mice (≧6-week-old) were paired with 3- to 4-month-old wild-type females for at least 2 months. Mating cages typically consisted of one male and one female. The presence of vaginal plugs was checked, and the pregnancy of females and the number of pups were recorded.

Spermatozoa counting

The mice were sacrificed and sperm were collected from the cauda epididymis in 37°C phosphate-buffered saline (PBS) solution and fixed for 15 min at room temperature with 4% formaldehyde. Cells were counted using a hemocytometer chamber under a light microscope, and sperm number was calculated by standard methods.

Spermatozoa motility analysis

Sperm were collected after swimming out from the cauda epididymis in warm PBS. Sperm motility was observed using an inverted microscope (Nikon, Tokyo, Japan) equipped with 10× objective. Movies were recorded at 15 frames/sec with a SANYO (Osaka, Japan) color charge-coupled device, high-resolution camera (VCC-3972), and Pinnacle Studio HD (version 14.0) software. For each sample, 10 fields were analyzed. Individual spermatozoa were tracked using Image J (National Institutes of Health, Bethesda, MD) and the plug-in MTrackJ. Sperm motility was calculated as a curvilinear velocity (VCL), which is equivalent to the curvilinear distance (DCL) traveled by each individual spermatozoon in 1 s (VCL = DCL/*t*).

Histology on tissue sections

Testes and epididymides of adult mice were fixed in 4% formaldehyde solution in PBS for at least 24 h, paraffin embedded, and 5 μm sections were stained with hematoxylin and eosin, using standard procedures. Slides were examined using a BX51 Olympus microscope (Olympus Corp., Melville, NY; Center Valley, PA), and photographs were taken with a ProgRes C14 camera (Jenoptik Laser, Jena, Germany).

Western blot analysis

Tissue samples from 3- to 4-month-old mice were homogenized in lysis buffer (50 mM Tris–HCl, pH 8.0; 170 mM NaCl; 1% NP40; 5 mM EDTA; 1 mM DTT; and protease inhibitors (Complete mini; Roche diagnostics GmbH, Mannheim, Germany)) using Ultra Turrax and collecting supernatants after centrifuged at 13,000 rpm for 10 min at 4°C and using Bio-Rad DCTM protein assay kit (Bio-Rad, Hercules, California, USA) to test the protein concentration by Lowry assay. Protein samples were denatured at 95°C for 10 min, then separated by SDS-PAGE and transferred onto polyvinylidene fluoride membranes (Millipore, Billerica, MA). The membranes were then soaked in a Tris-buffered saline solution, containing 5% nonfat milk powder and 0.05% Tween 20 and blocked for at least 1 h. The membranes were incubated with indicated antibodies (Anti-COPS5/JAB1: Sigma, St. Louis, MO, USA, 1:2,000, Cat No: J3020; β-actin: Cell Signaling Technology, 1:2,000, Cat No: 4967 S; PARP: Cell Signaling Technology, 1:2,000, Cat No: #9542; Caspase-3: Cell Signaling Technology, Boston, MA, USA, 1:2,000, Cat No: #9665; FANK1: Santa Cruz Biotechnology, Dallas, Texas, USA, 1:1,000, Cat No: SC-398057; sperm acrosome associated 1 (SPACA1), 1:4,000, produced by Dr. Oko's laboratory at Queen's University, Canada; GAPDH: Santa Cruz Biotechnology, 1:2,000, Cat No: SC-32233; Anti-IFT20: 1:2,000, produced by Dr. Gregory Pazour's laboratory at the University of Massachusetts Medical School, Table 1) at 4°C overnight, washed three times with Tris-buffered saline solution containing 0.05% Tween 20 (TBST), and then incubated at room temperature with secondary antibody at a dilution of 1:2,000 for at least 1 h. After washing with TBST twice and lastly washing with TBS, the bound antibodies were detected with Super Signal Chemiluminescent Substrate (Pierce, Rockford, IL).

Table 1. Antibody information.

Name	Catalogue number	Purpose	Dilution
Anti-COPS5/JAB1	J3020, SIGMA	Western blot	1:2000 for western blot; 1:200 for IF
β-Actin	4967 S, Cell Signaling Technology	Western blot	1:2000
PARP	#9542, Cell Signaling Technology	Western blot	1:2000
Caspase-3	#9665, Cell Signaling Technology	Western blot	1:2000
FANK1	SC-398057, Santa Cruz Biotechnology	Western blot	1:1000
SPACA1	Dr. Oko's Laboratory	Western blot	1:4000
GAPDH	SC-32233, Santa Cruz Biotechnology	Western blot	1:2000
Anti-IFT20	Dr. G.J.P.'s Laboratory	Western blot	1:2000 for western blot; 1:200 for IF
Anti-α-tubulin	T9026-2ML, SIGMA	IF	1:200
Anti-SOX9	ab185966, Abcam	IF	1:200
Anti-rabbit IgG	711166152, Jackson ImmunoResearch	IF	1:200
Anti-mouse IgG	DI-2488, Vector Laboratories	IF	1:400

TUNEL staining analysis

The paraffin-embedded testis sections were heated at 60°C for 1 h. Then the samples were deparaffinized with xylene twice and washed with 100% ethanol twice. After rehydrating with 70% ethanol for 5 min and 35% ethanol for 5 min, the slides were incubated with 3% H_2O_2 in methanol at room temperature for 20 min. Afterward, the sections were incubated and labeled following the manufacturer's instructions for the In Situ Cell Death Detection Kit (Roche, cat. No.11684795910). Identical protocol and reagent catalog numbers of double labeling of presumed apoptotic cells with fragmented DNA and Sertoli cell marker SOX 9 (Abcam, ab185966) were used as described in previous studies [60]. The only difference is new camera used for acquisition: Retiga QI-R6 camera (Teledyne QImaging, Surrey, BC, Canada) operated by MetaMorph 7.10.2.240 software (Molecular Devices, San Jose, CA).

Plasmid transfection, immune-fluorescence, and coimmunoprecipitation assays

To test the colocalization of mouse COPS5 and mouse IFT20 in CHO cells, full-length *Cops5* was amplified using the same primer set as to make the yeast expression construct, and the cDNA was cloned into pEGFP-N2 vector. FLAG-tagged IFT20 plasmid was provided by Dr. Gregory Pazour at University of Massachusetts. IFT20/FLAG and COPS5/GFP were cotransfected into the CHO cells using the transfection kit according to the manufacturer's instructions. After culturing the cells for another 2 days, the medium was discarded and the cells were washed with PBS once more. Then the cells were fixed and permeabilized with methanol at −80°C for 7 min. The samples were washed three times with PBS and blocked with 10% goat serum for 30 min at 37°C. Then the samples were incubated overnight with the primary antibody (Anti-Flag: Sigma, 1:200, Cat No: F3165-2MG). Following secondary antibody ($Cy^{TM}3$ AffiniPure F $(ab')_2$ Fragment Donkey Anti-Rabbit IgG (H + L): Jackson ImmunoResearch, 1:200, Cat No: 711166152; DyLight 488 Horse Anti-Mouse IgG Antibody: Vector Laboratories, Burlingame, CA, 1:400, Cat No: DI-2488) incubation, the slides were washed three times with PBS and mounted using VectaMount with 4′, 6-diamidino-2-phenylindole (DAPI) (Vector Laboratories) and sealed with a cover slip. Images were captured by a confocal laser-scanning microscopy (Zeiss LSM 700).

To conduct coimmunoprecipitation (co-IP) assay, plasmids expressing IFT20/Flag and COPS5/GFP were cotransfected into COS-1 cells, and co-IP assay was performed following previously described methods [61]. Briefly, the supernatant of cell lysates was precleaned with protein A beads at 4°C for 30 min, and the precleared extract was then incubated with the anti-Flag antibody or normal mouse IgG as a negative control at 4°C for 2 h. The mixture was then incubated with protein A beads at 4°C overnight. The beads were washed with immunoprecipitation buffer (50 mM NaCl, 50 mM Tris-HCl, pH 8.0, 5 mM EDTA, 1% Triton X-100, 1 mM PMSF, proteinase inhibitor) three times. The collected samples were then subjected to Western blot analysis with an anti-Flag antibody and an anti-GFP antibody (Roche, 1:1000, Cat No: 11814460001).

Isolation of spermatogenic cells and immunofluorescence analysis

Testes were separated from 3–4 month mice and incubated in a 15-mL centrifuge tube with 5-mL DMEM containing 0.5 mg/mL collagenase IV and 1.0 μg/mL DNase I (Sigma-Aldrich) for 30 min at 32°C and shaken gently. Then the testes were washed once with PBS after centrifugation at 1,000 rpm for 5 min under 4°C and the supernatant was discarded. Afterward, the cell pellet was fixed with 5 mL paraformaldehyde containing 0.1 M sucrose and shaken gently for 15 min at room temperature. After washing three times with PBS, the cell pellet was resuspended with 2 mL PBS and loaded on positively charged slides. The slides were stored in a wet box at room temperature after air drying. Afterward, the spermatogenic cells were permeabilized with 0.1% Triton X-100 (Sigma-Aldrich) for 5 min at 37°C. Finally, the samples were incubated overnight with the primary antibody (Anti-COPS5/JAB1: Sigma, 1:200, Cat No: J3020; Anti-IFT20: 1:200, produced by Dr. Gregory Pazour's laboratory at the University of Massachusetts Medical School). Images were also captured by a confocal laser scanning microscopy (Zeiss LSM 700).

Transmission electron microscopy

Mouse testes tissues were fixed in 3% glutaraldehyde/1% paraformaldehyde in 0.1 M sodium cacodylate, pH 7.4 at 4°C for overnight and processed for electron microscopy. Images were taken with a Jeol JEM-1230 transmission electron microscope.

Results

COPS5 is a binding partner of IFT20

A direct yeast two-hybrid assay was conducted to confirm the interaction between IFT20 and COPS5. Like the positive control,

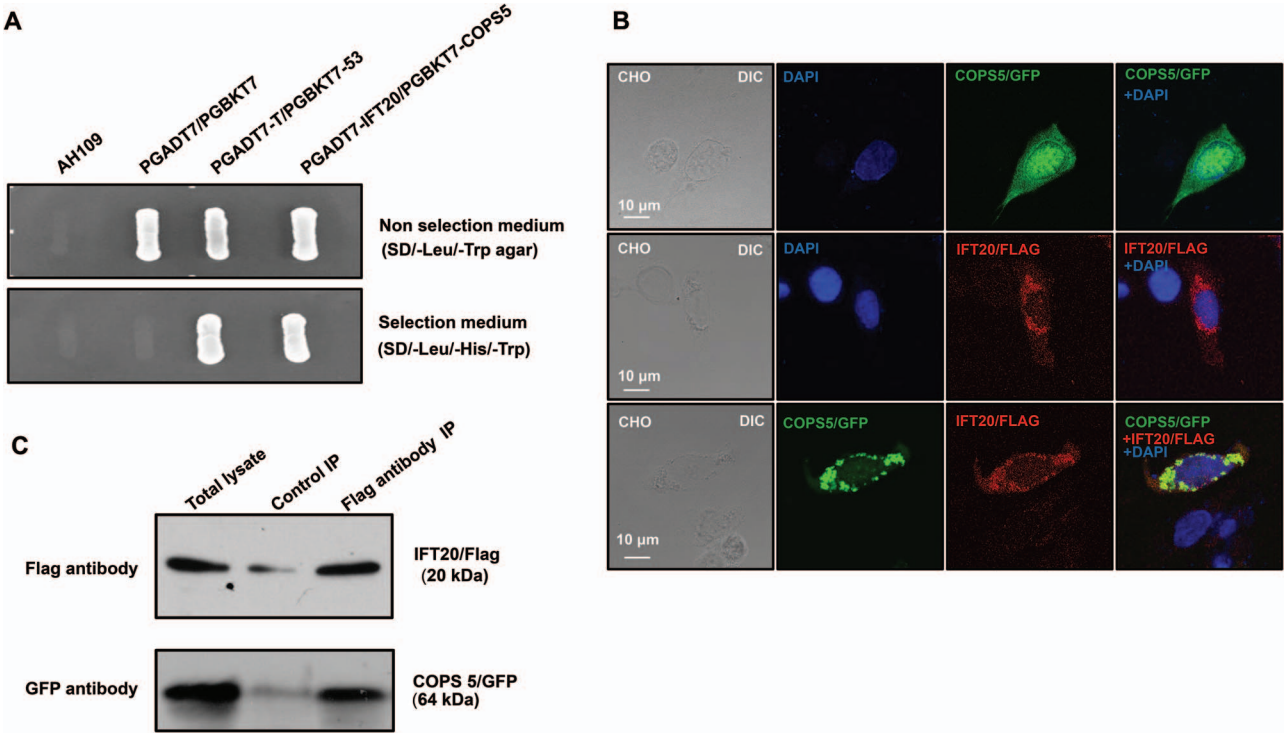

Figure 1. Identification of COPS5 as a binding partner of IFT20, a major spermatogenesis regulator. A. IFT20 interacts with COPS5 in yeast. Pairs of indicated plasmids were cotransformed into AH109 yeast, and the transformed yeast were grown on either selection plates (lacking tryptophan, leucine, and histidine) or nonselection plates (lacking tryptophan and leucine). Notice that all the yeast except AH109 grew on the nonselection plate. Yeast expressing IFT20/COPS5 and P53/large T antigen pairs grew on selection plate. B. COPS5 colocalizes with IFT20 in CHO cells. When expressed alone, COPS5 was present in the whole cells, and IFT20 as vesicles. When the two proteins were coexpressed, COPS5 was present as cytoplasmic vesicles and colocalized with IFT20. C. Coimmunoprecipitation of COPS5 with IFT20. COS-1 cells were cotransfected with COPS5/GFP and IFT20/Flag. The cell lysate was immunoprecipitated with anti-Flag antibody and then subjected to Western blot analysis with anti-FLAG and anti-GFP antibodies. The cell lysate immunoprecipitated with a mouse normal IgG was used as a control. The anti-Flag antibody pulled down both IFT20/Flag and COPS5/GFP.

the yeast cotransformed with the two plasmids expressing COPS5 and IFT20 grew on the selection medium (Figure 1A), indicating that the two proteins interact in yeast. To further examine interaction of the two proteins, CHO cells were transfected with the plasmids expressing the two proteins. When the CHO cells expressed COPS5 only, the protein was present in the entire cell body (Figure 1B, upper panel). IFT20 was present as cytoplasmic vesicles (Figure 1B, middle panel). However, when CHO cells expressed both proteins, COPS5 was only present in cytoplasmic vesicles and colocalized with IFT20 (Figure 1B, lower panel). In addition, we transfected COS-1 cells with COPS5/GFP and IFT20/Flag expression plasmids and conducted a coimmunoprecipitation assay. The Flag antibody pulled down both Flag-tagged IFT20 and COPS5, suggesting an interaction between two proteins (Figure 1C).

COPS5 is highly expressed in the testis but not epididymal sperm and is present in unique organelles in male germ cells

COPS5 tissue distribution was examined by Western blot analysis. The protein was only detected in the testis, spleen, and brain when a less sensitive visualizing system was used (Figure 2A. upper panel). However, when a more sensitive system was used, it was found that COPS5 was present in most tissues examined, except kidney (Figure 2A, middle panel). Even though COPS5 was highly expressed in the testis, the protein was not detected in epididymal sperm (Figure 2B). Expression of COPS5 during the first wave of spermatogenesis was also analyzed. The protein was expressed as early as 8 days after birth, and the level was increased with age (Figure 2C). Localization of COPS5 in male germ cells was investigated in isolated germ cells. The protein was present in the cytoplasm of spermatocytes, highly concentrated in acrosomes of round and elongating spermatids and in the manchette of elongating spermatids (Figure 2D).

Inactivation of mouse *Cops5* gene resulted in infertility associated with significantly reduced testis weight and sperm number

High expression of COPS5 in the testis, particularly in germ cells, suggests a role for this gene in spermatogenesis. To examine a potential role, the floxed *Cops5* mice were crossed to *Stra8-iCre* mice so that the *Cops5* gene was specifically disrupted in male germ cells (*Cops5* KO). Genotyping using specific primer sets indicated that homozygous mutant mice were obtained (Supplemental Figure S1). Examination of total testicular COPS5 protein expression by Western blot revealed that only a trace amount of COPS5 was present in the knockout mice (Figure 3A). The homozygous knockout mice were grossly normal, and fertility of 2-month-old control and mutant mice were evaluated by breeding to wild-type 3- to 4-month-old females with normal fertility. All mice tested showed normal mating behavior, and vaginal plugs were observed in the females. However, through 2 months of breeding test, even though seven

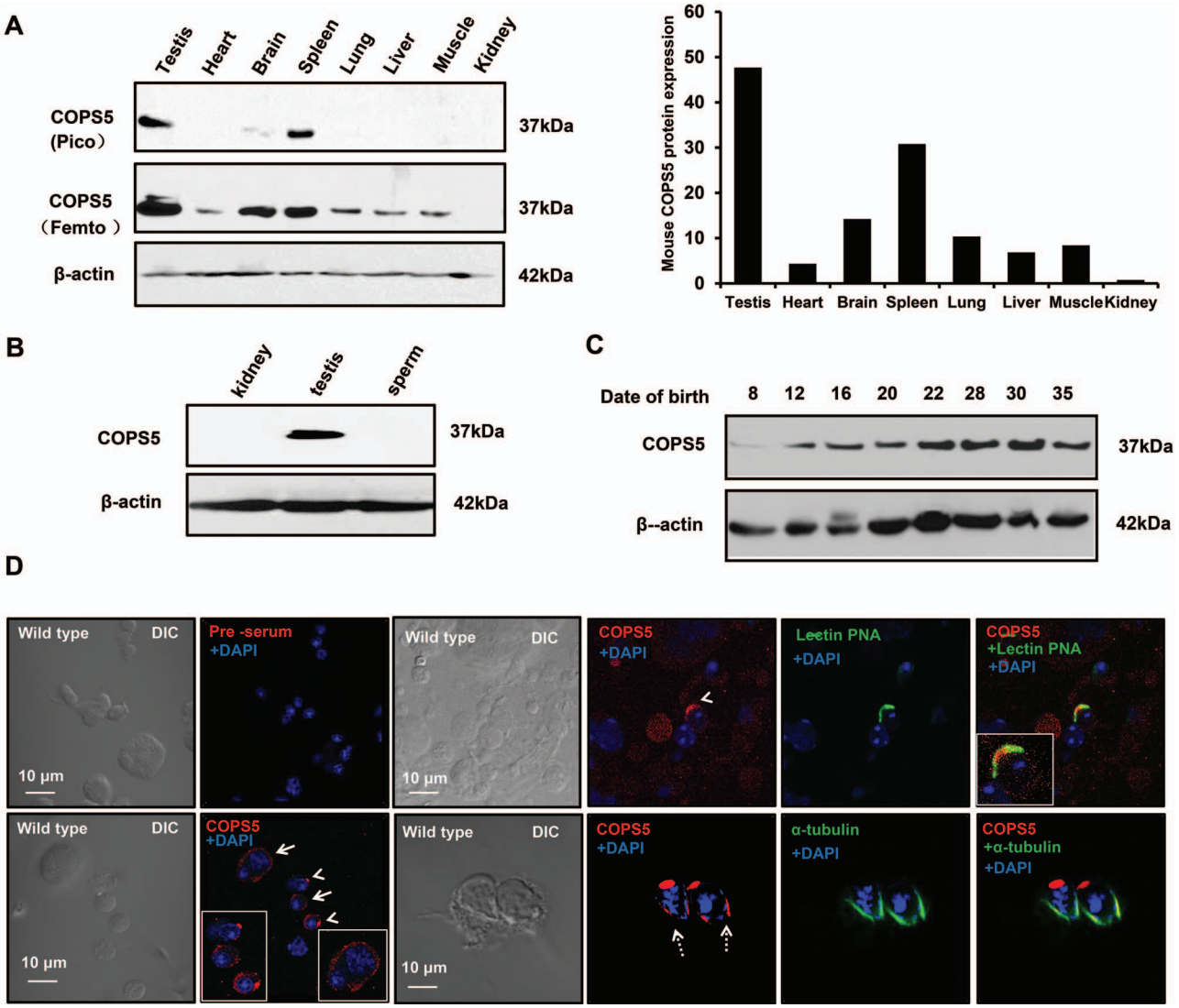

Figure 2. Tissue distribution of COPS5 and its localization in male germ cells. A. Analysis of tissue distribution of mouse COPS5 protein by Western blot. Left: representative Western blot results. When using a low-sensitivity Pico system, COPS5 was only detected in the testis, spleen, and brain (upper panel). When using a high-sensitivity Femto system, COPS5 was also detected in other somatic tissues, except kidney (middle panel). β-Actin was analyzed as a loading control (bottom panel). Right: relative COPS5 protein expression levels normalized to β-actin. B. COPS5 is not expressed in the epididymal sperm. Epididymal sperm were collected from cauda epididymis, and Western blot was conducted. COPS5 protein was detected in the testis, but not sperm. C. Testicular COPS5 expression levels during the first wave of spermatogenesis. COPS5 was detectable from day 8 after birth; its expression was up-regulated at day 12, and further increased from day 22 after birth. D. Examination of COPS5 localization in normal male germ cells. Testicular cells were isolated, and immunofluorescence staining was conducted. COPS5 signal was observed in the cytoplasm of spermatocytes (arrow); it localizes on the acrosome of round (arrow heads) and elongating (dotted arrows) spermatids. In elongating spermatids, COPS5 also localizes in the manchette.

control mice showed normal fertility, none of the seven homozygous mutant mice sired any pups/litters (Table 2). Testis weight and testis weight/body weight were significantly reduced in the homozygous mutant mice (Figure 3B). The cauda epididymal sperm counts were dramatically reduced in the mutant mice (Table 2). Only a few sperm were present in the knockout mice and most of them showed abnormal morphology (Figure 3C and D), and sperm motility was significantly reduced (Figure 3E and F, Supplemental Movies S1).

Impaired spermatogenesis in the *Cops5* KO mice

Testes weights and cauda epididymal sperm counts were significantly reduced in *Cops5* knockout mice, indicating an impairment of spermatogenesis. Therefore, morphology of the testes and epididymides in adult control and *Cops5* mutant mice was examined. In control mice, the seminiferous tubules showed normal spermatogenesis (Figure 4A, upper panel), and the cauda epididymal lumen was filled with mature spermatozoa (Figure 4B, upper panel; Supplemental Figure S3, left). In the *Cops5* knockout mice, seminiferous tubule structure was completely disrupted and elongating spermatids were rarely observed (Figure 4A, lower panel; Supplemental Figure S2). In some mice, the epididymal lumen was devoid of mature sperm; instead, some abnormal germ cells were present (Figure 4B, lower panel). In other mutant mice, some sperm with normal morphology were discovered in the epididymal lumen, but their density was dramatically lower than that of the control mice (Supplemental Figure S3, right).

Table 2. Fertility, fecundity, and sperm count of control and conditional *Cops5* mutant mice. To test fertility, adult and 6-week-old males were bred with wild-type females for at least 2 months. Litter size was recorded for each mating and sperm number was counted.

Genotype	Male fertility	Litter size (n = 7)	Sperm count (10^6, n = 10)
Control	7/7	7.14 ± 1.77	10.2 ± 2.88
Cops5 KO	0/7	0	0.47 ± 0.96

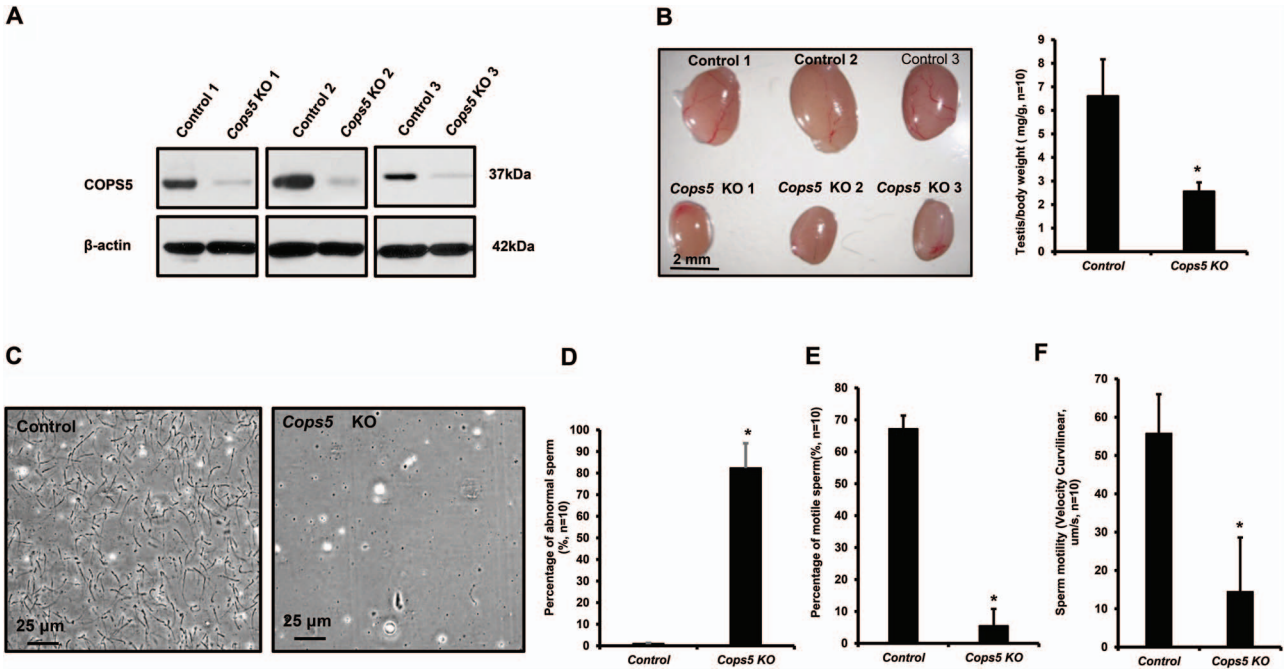

Figure 3. Significantly reduced testis weight, sperm number, motility, and abnormally formed sperm in the conditional *Cops5* knockout mice. A. Representative Western blot result showing only a trace amount of COPS5 protein was expressed in the testes of *Cops5* conditional knockout mice (n = 3). B. Significantly reduced testis size in the *Cops5* knockout mice. Left: representative image of testes from three control and three conditional *Cops5* knockout mice. Right: mean testis/body weight of the control and knockout mice, showing a statistically significant reduction in weight (*), $P < 0.05$. C. Representative images of epididymal sperm from a control mouse and a conditional *Cops5* knockout mouse. D. Significantly increased percentage of abnormal sperm in the *Cops5* mutant mice (n = 10). E, F. Percentage of motile sperm and sperm motility was reduced in the conditional *Cops5* knockout mice (n = 10). Statistically significant differences (*); $P < 0.05$.

Depletion of COPS5 caused significantly increased apoptosis and reduced FANK1 expression

Histological examination of the testis in *Cops5* knockout mice revealed a significant loss of germ cells, by what appeared to be apoptosis. To test this hypothesis, TUNEL staining was conducted on testes sections from control and *Cops5* knockout mice. As a negative control, the section was not incubated with fluorescence probe (Figure 5A, panel a); as a positive control, the section was treated with DNAse I, and almost all cells were positive (Figure 5A, panel b). In the control mice, only an occasional apoptotic cell was seen in the seminiferous tubules (Figure 5A, panel c). However, the numbers of TUNEL-positive cells in the *Cops5* knockout mice was significantly increased (Figure 5A, panel d). To distinguish the cell type of the apoptotic cells, a Sertoli cell marker SOX 9 was double labeled of presumed apoptotic cells with fragmented DNA. It showed that DNA fragmentation appears solely in germ cells and not in the neighboring Sertoli cells, near/within adluminal compartment of the seminiferous tubules (Figure 5B). The level of apoptosis was further examined by Western blot analysis using two antibodies, anti-poly (ADP-ribose) polymerase-1 (PARP), a protein that helps cells to maintain viability, and anti-Caspase-3, a critical inducer of apoptosis. PARP expression level was dramatically reduced in the *Cops5* knockout mice; however, in contrast, Caspase-3 expression level was significantly increased (Figure 5C). FANK1 is another factor that is known to inhibit apoptosis in male germ cells, and its knock-down [47] resulted in a phenotype similar to that in the present study of *Cops5* knockout mice. Therefore, because FANK1 is reportedly a COPS5 binding partner [46], we also examined testicular FANK1 expression levels in the *Cops5* knockout mice. Compared to the control mice, FANK1 expression level was dramatically reduced in the knockout mice (Figure 5D).

Acrosome biogenesis was affected in the absence of COPS5

Even though there was a significantly increased number of apoptotic germ cell in the seminiferous tubules, some germ cells were able to complete meiosis and develop into round spermatids and even a few elongated spermatids. Because COPS5 is present in the acrosome of round and elongating spermatids, we examined acrosome biogenesis in the knockout mice. Testicular cells, isolated from control and *Cops5* knockout mice, were double stained with an anti-COPS5 antibody and lectin peanut agglutinin (PNA),

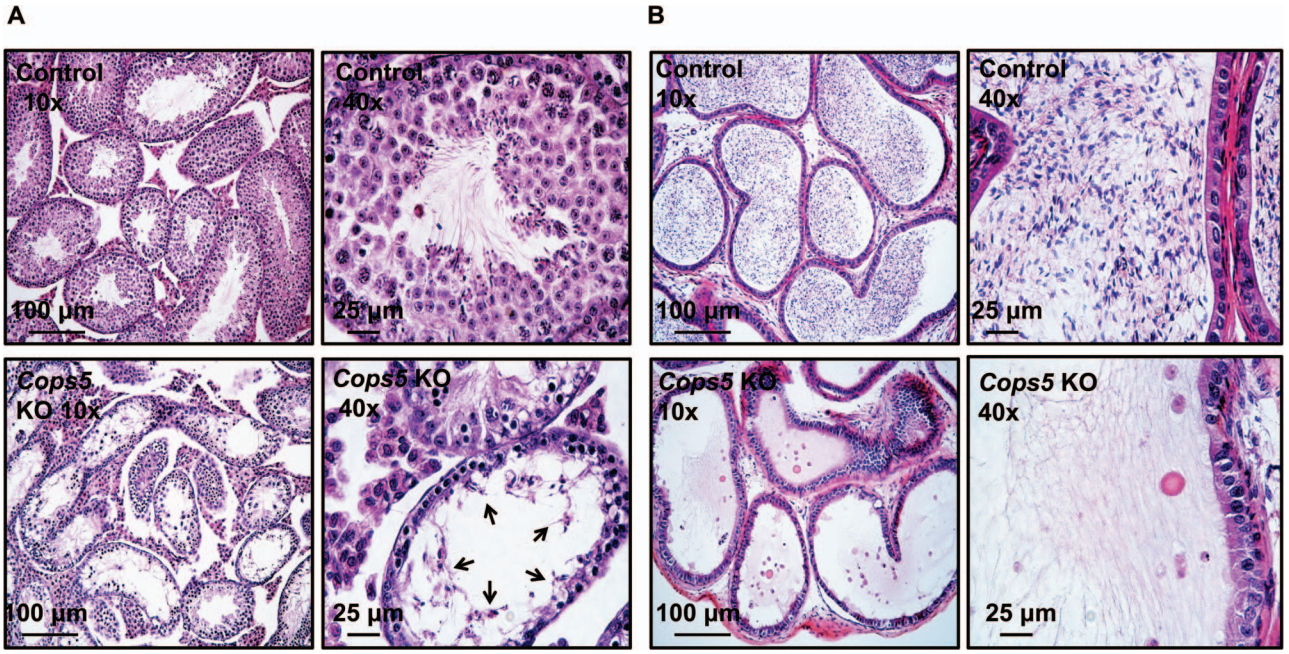

Figure 4. Abnormal spermatogenesis and loss of cauda epididymal sperm in the conditional *Cops5* knockout mice. A. Representative histology of testis. Normal spermatogenesis can be observed in the images of control mice (upper panels). The lower panels show abnormal spermatogenesis in the *Cops5* knockout mice. A number of degenerating germ cells (arrows) are seen in the lumen of seminiferous epithelium exhibiting severe hypospermatogenesis, with very few developed elongated spermatids. B. Representative histology of epididymis. In the control cauda epididymis (upper panel), numerous mature sperm were stored in the lumen. In the knockout mice (lower panels), round bodies (possibly sloughed germ cells) and cellular debris were seen with the rare developed sperm.

an acrosome marker. In the control mice, both COPS5 antibody and PNA-lectin positively stained spermatids and the two signals were colocalized (Figure 6A, upper panel). However, in the *Cops5* knockout mice, not only was the COPS5 signal absent, the lectin PNA signal for the acrosome was also absent in the spermatids (Figure 6A, lower panel). The expression of SPACA1, an acrosome component [62], was also examined by Western blot analysis, and its level was significantly reduced in the *Cops5* knockout mice (Figure 6B).

COPS5 determines IFT20 expression level and localization in male germ cells, but its localization and expression was not changed in the *Ift20* knockout mice

The interaction between COPS5 and IFT20 propelled us to further examine the functional relationship of these two proteins *in vivo*. We first compared IFT20 expression levels and localization in the control and *Cops5* knockout testes. Western blot analysis revealed that testicular IFT20 expression level was significantly reduced in the *Cops5* knockout mice (Figure 7A). Immunofluorescence staining demonstrated that in the control mice, IFT20 was present in Golgi bodies of spermatocytes and the acrosomes of round spermatids (Figure 7B, left panel). However, in *Cops5* knockout mice, even though IFT20 was still present in the Golgi bodies of spermatocytes (Figure 7B, middle panel), the protein was no longer localized in the acrosome of round spermatids; instead, it was present as individual vesicles in the cytoplasm (Figure 7B, right panel). COPS5 expression level and localization were also examined in the *Ift20* knockout mice (*Ift20* KO). Western blot result showed that COPS5 expression level was comparable between the control and *Ift20* KO (Figure 7C). As in the control mice, COPS5 was still localized in the acrosome in the *Ift20* KO mice (Figure 7D).

Ultrastructural changes in the seminiferous tubules of the COPS5 knockout mice

To investigate the structural basis for the molecular changes observed in the absence of COPS5, the seminiferous tubule ultrastructure was examined. In control mice, the acrosome was well formed in round and elongating spermatids (Figure 8A and B). In *Cops5* KO, significant numbers of apoptotic cells were also present in the *Cops5* KO testis (Figure 8C), with evidence of Sertoli cell phagocytosis (Figure 8D). Acrosome formation was absent in most round spermatids (Figure 8E), and in other spermatids, an abnormal acrosome was formed or a very thin acrosome was attached to the Sertoli cell membrane by an abnormal ectoplasmic specialization (Figure 8F). Large vacuoles were present in the epithelium and were presumably the spaces remaining after Sertoli cell phagocytosis of the apoptotic cells (Figure 8G). The few germ cells that developed into elongating spermatids had abnormal nuclei (Figure 8H).

Discussion

IFT is a highly conserved mechanism for cilia formation [63]. Our laboratory analyzed the roles of several IFT components in the formation of sperm, which have the typical "9 + 2" motile axonemal complex [64], and discovered that these IFTs were essential for male fertility and sperm formation [56–59]. To explore the mechanisms underlying these important functions, we did yeast two-hybrid screen using IFT components as bait. COPS5 was identified as a major

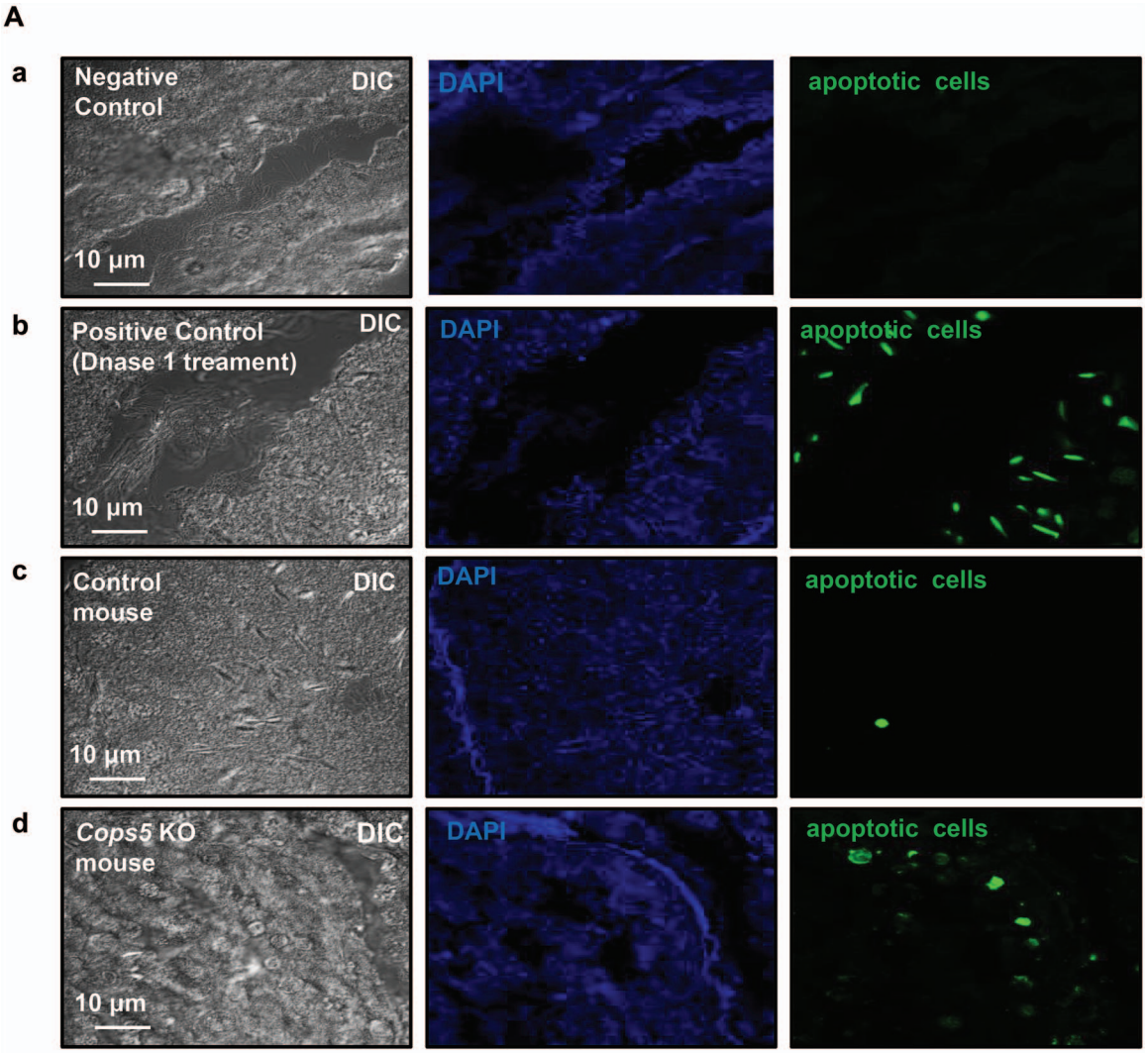

Figure 5. Depletion of COPS5 caused significantly increased apoptosis and reduced FANK1 expression. A. Examination of apoptosis in the testes of a control mouse and a *Cops5* knockout mouse by TUNEL staining. Green signal indicates the apoptotic cells. Negative control (panel a): the control testis section was not incubated with fluorescent probe; positive control (panel b): the control testis section was treated with DNase 1, and incubated with fluorescent prove; few apoptotic cells were present in the control mouse (panel c); increased number of apoptotic germ cells were observed in the *Cops5* knockout mice (panel d). B. Double labeling of presumed apoptotic cells with fragmented DNA (green; TUNEL labeling) and a Sertoli cell marker SOX 9 (red; immunofluorescence) in the wild type (A) and KO (B, C) mice. (A, B) By exclusion, DNA fragmentation appears solely in germ cells and not in the neighboring Sertoli cells, near/within adluminal compartment of the seminiferous tubules. (C) Fluorescence channel-separated detail of TUNEL-positive cells shown in panel B, including the grayscale-rendered labeling of SOX9 (C), TUNEL (C′), and total DNA counterstained by DAPI (C″), and a merged pseudo-colored image (C‴). C. Testicular expression levels of PARP and active Caspase 3 in control and *Cops5* knockout mice by Western blot analysis (n = 3). Decreased PARP and increased active Caspase 3 expression were observed in the *Cops5* knockout mice. $P < 0.05$ (*). D. Examination of testicular FANK1 expression (n = 3). FANK1 expression level was dramatically reduced in the *Cops5* knockout mice. (*) $P < 0.05$.

binding partner of IFT20. Interaction between IFT20 and COPS5 was further confirmed by colocalization and co-IP experiment *in vitro*. In colocalization assay, even though COPS5 only was present in the whole cell body, it was only present in the cytoplasmic vesicles and exactly colocalized with IFT20 when IFT20 was coexpressed. This strongly indicates that the two proteins interact and IFT20 drives COPS5 to the cytoplasmic vesicles. Therefore, we decided to further investigate the function of this gene in male fertility and spermatogenesis. Even though COPS5 has been shown to play important roles in many other somatic systems, the highest level of its protein expression among the tissues examined was in testis, indicating a particularly important role in male fertility, which was subsequently confirmed in the male germ cell-specific knockout mice as described here.

During the first wave of spermatogenesis, COPS5 protein was expressed throughout the entire spermatogenesis process. Weak COPS5 signal was present in the cytoplasm of spermatocytes. In round spermatids, it was localized in the acrosome; in elongating spermatids, it was present in both the acrosome and manchette, which are unique structures present only in male germ cells [65]. Given that IFT20 is also present in the acrosome and manchette and is essential for spermiogenesis, the pattern of COPS5 localization strongly suggested that COPS5 has a function that could be related to IFT20. Testicular expression level of IFT20 was significantly

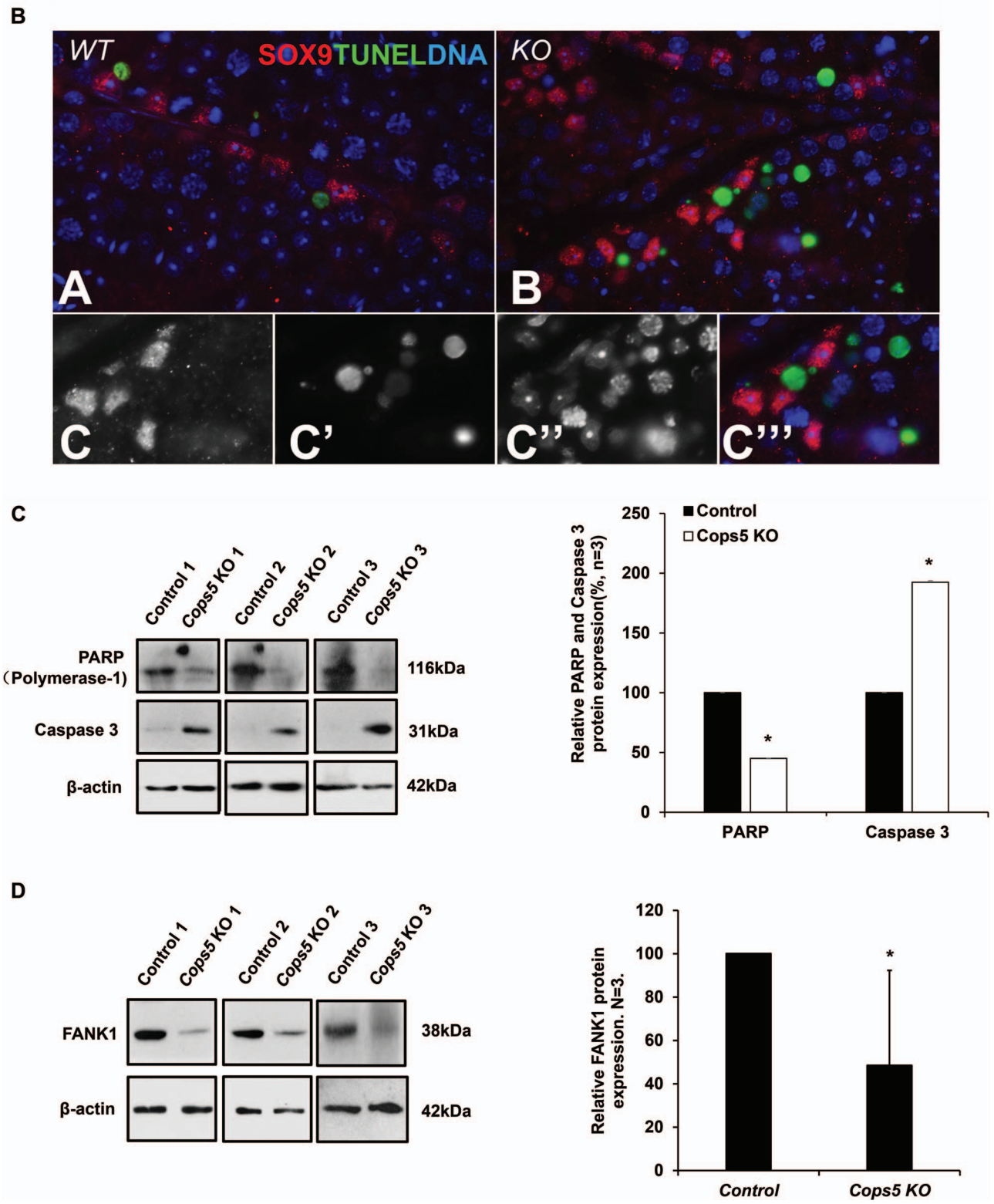

Figure 5. Continued.

reduced in the *Cops5* knockout mice. IFT20 localization was also changed in the *Cops5* knockout mice. Even though IFT20 was still present in Golgi vesicles in the *Cops5* knockout mice, it was no longer present in the acrosome of round spermatids. Instead, the IFT20 signal was scattered near the location where the acrosome should form. Reduced IFT20 expression level in the *Cops5* knockout mice might be caused by degradation of the protein due to instability in the absence of COPS5. Acrosome formation was also affected as

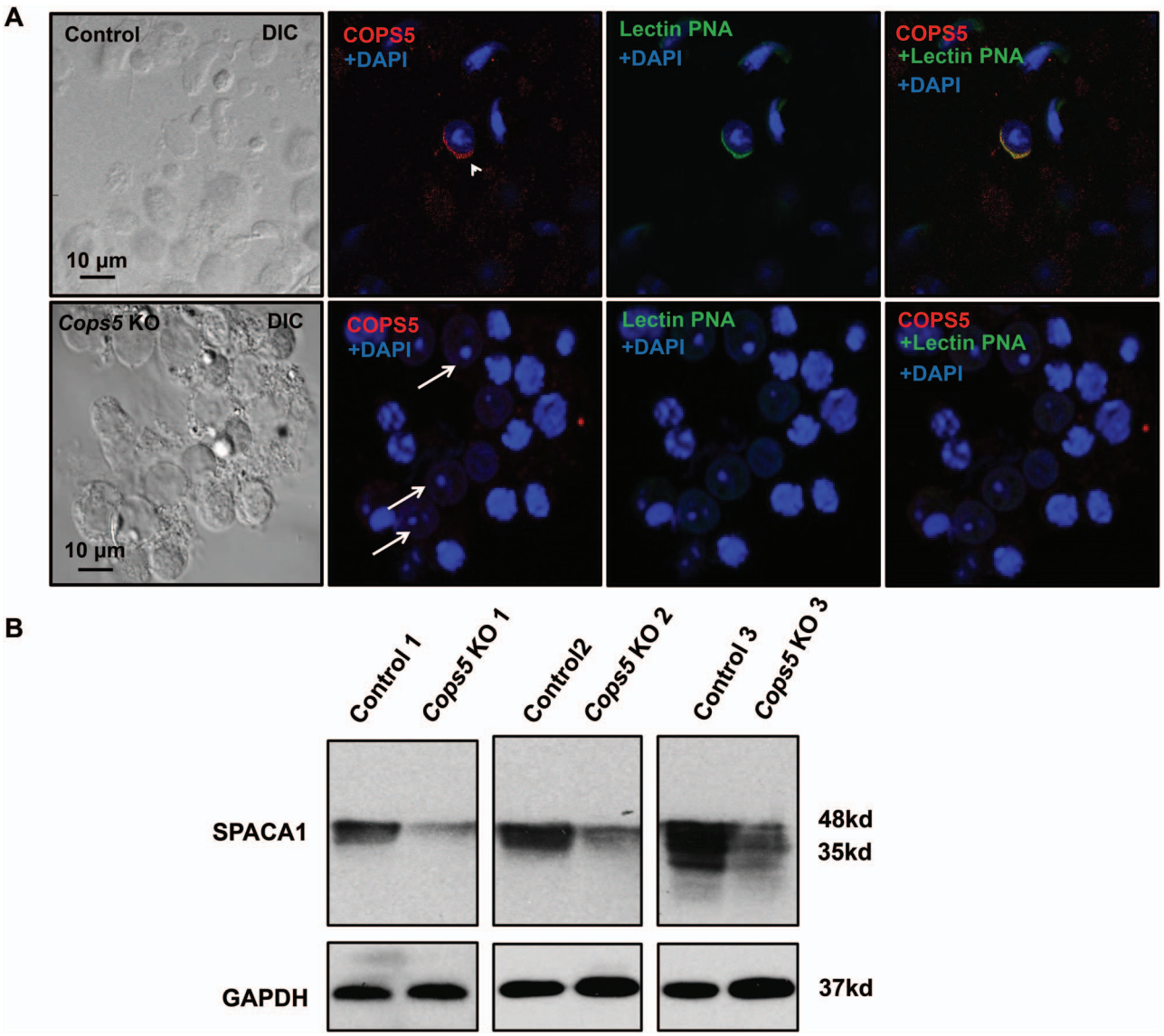

Figure 6. Acrosome biogenesis was affected in the absence of COPS5. **A.** Representative images of testicular cells isolated from control (upper panel) and *Cops5* knockout mice (lower panel) stained with specific anti-COPS5 antibody (red) and the acrosome marker peanut-lectin PNA (green). Acrosome staining was observed in spermatids from the control germ cells (arrow head), but no peanut-lectin staining was observed in spermatids (white arrows) of the *Cops5* knockout mouse. B. Expression level of SPACA1 protein, a marker of acrosome, was examined by Western Blot. Compared with controls, there was an obviously decreased expression of SPACA1 protein in the *Cops5* mutant mouse testis.

evaluated by specific acrosome staining and TEM examination. In contrast, COPS5 expression level and localization was not changed in the testis-specific IFT20 knockout mice. It appears that COPS5 is an upstream player of IFT20 and determines IFT20 localization on the acrosome. In the conditional *Ift20* knockout mice, acrosome formation was not affected [56]. In somatic cells, IFT20 is involved in vesicle trafficking through Golgi bodies toward centrioles [66], which function as the template for cilia formation [67]. In male germ cells, IFT20 is on the acrosome surface, and the localization appears to be dependent on other proteins. Thus, failure of IFT20 localization in the acrosome area in *Cops5* KO males might be either a direct effect due to absence of COPS5, or a secondary effect of disrupted acrosome formation in the absence of COPS5. Given that very few cells developed into elongating spermatids in the *Cops5* knockout mice, it is not known if COPS5 is also essential for manchette formation/function and IFT20 localization in the manchette. Due to extremely low sperm count in the conditional *Cops5* knockout mice, we were not able to further analyze epididymal sperm. We expect that most epididymal sperm from the knockout mice have no or an abnormal acrosome.

A more striking phenotype was the dramatic increase in the presence of apoptotic cells in seminiferous tubules. Normal spermatogenesis requires a well-organized cell population within the seminiferous tubules [68]. Up to 75% of germ cells undergo apoptosis in the seminiferous tubules to keep the balance [69]. Disruption of the balance between cell survival and apoptosis has been demonstrated to impair spermatogenesis, which can lead to male infertility

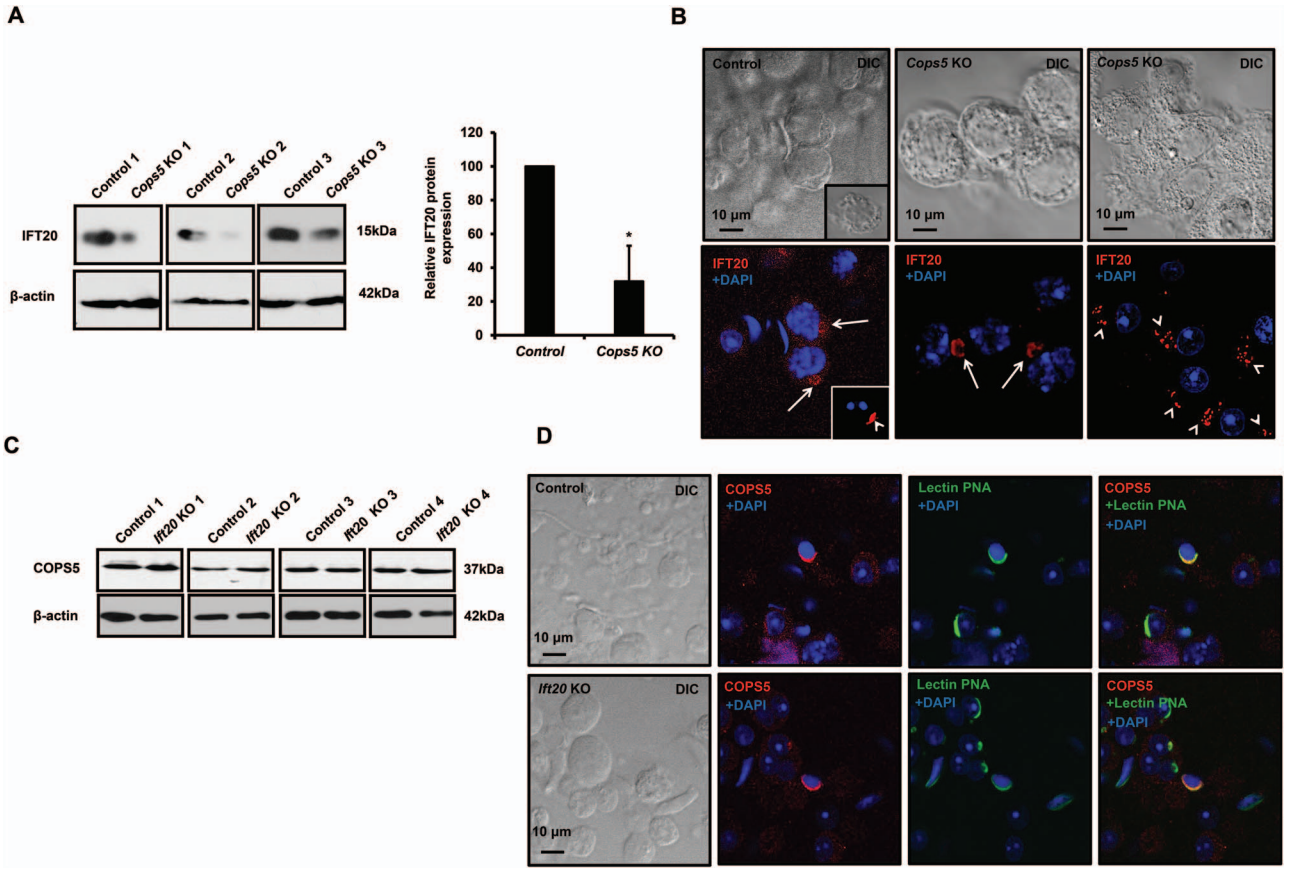

Figure 7. COPS5 determines IFT20 expression level and localization in male germ cells, but COPS5 localization and expression were not changed in the *Ift20* knockout mice. A. Analysis of testicular IFT20 expression in control and *Cops5* knockout mice by Western blot. The expression level of IFT20 was reduced remarkably in the knockout mice (n = 3). B. IFT20 localization in germ cells of the control and *Cops5* knockout mice by immunofluorescence staining (red). IFT20 was localized in the Golgi body of a spermatocyte (arrows) and acrosome of a round spermatid (arrow heads). In the *Cops5* knockout mouse, IFT20 was still present in the Golgi body of the spermatocyte but was no longer seen in the spermatid acrosome. However, the protein was present as small vesicles near one side of the nucleus. C. Expression levels of COPS5 in control and *Ift20* conditional knockout mice. Compared with control mice, there was no change in the COPS5 expression level; D. COPS5 was still present in the acrosome of spermatids from the *Ift20* knockout mice. The testicular cells were double stained with COPS5 antibody (red) and the acrosome marker lectin PNA (green). Like in the control mouse, COPS5 was still present in the acrosome. Unlike the *Cops5* knockout mice, acrosome staining was not affected in the *Ift20* knockout mice.

associated with azoospermia, asthenozoospermia, hypospermatogenesis, and oligozoospermia [70, 71].

Apoptosis, also called programmed cell death, is an evolutionarily conserved cell death process. In adult mammals, germ cell apoptosis is conspicuous during normal spermatogenesis, especially the first wave of spermatogenesis [72]. Apoptosis is a choice to control germ cell number and eliminate defective GCs during testicular development and spermatogenesis [73]. Two major pathways, the mitochondrial pathway and the cell death receptor pathway, are involved in mammalian apoptosis. Recently, another novel pathway caused by UPR (unfolded protein response) in response to ER (endoplasmic reticulum) stress is also critical to germ cell elimination. Several growth factor candidates, such as KL (kit ligand, also known as SCF), bFGF (basic FGF), leukemia inhibitory factor, TGF-βs, forskolin, and RA (retinoic acid), were found to act as survival factors in the process of germ cell proliferation and differentiation [74–79]. Some testis-specific genes also contribute to germ cell apoptosis/survival, and these genes include *FANK1*, *RHBDD1*, *Spata17*, and *LM23* [55, 80–82]. Among these growth factors and genes, *FANK1*, also named Fibronectin type 3 and ankyrin repeat domains 1 protein, is of particular interest. FANK1 is a testis-specific transcriptional factor that controls germ cell apoptosis through regulation of apoptosis-related gene expression [53]. It has been shown that FANK1 is a COPS5 binding partner [54]. One mechanism for COPS5 to regulate germ cell apoptosis might be through the modulation of FANK1 expression.

Our study clearly demonstrated that COPS5 participates in at least two functions: (1) controlling germ cell survival/apoptosis and (2) acrosome biogenesis. How this protein plays such important roles in spermatogenesis remains to be determined. However, as documented in the introduction, COPS5 conducts multiple biological functions independently or as a cofactor of CSN [17, 18]. Of particular interest to the present study, the CSN complex is an essential regulator of the ubiquitin conjugation pathway [7, 8]. Protein ubiquitination is a posttranslational modification of proteins, which involves the attachment of ubiquitin [83]. During spermatogenesis, it has been shown that ubiquitination regulates the morphogenesis and function of organelles and structures in developing germ cells, including nuclear condensation, acrosome formation, and membrane trafficking [84–86]. Ubiquitination has also been associated with apoptosis [87]. It is noteworthy that FANK1 has been reported to be ubiquitinated *in vitro* [88]. Thus, it is possible that FANK1 undergoes

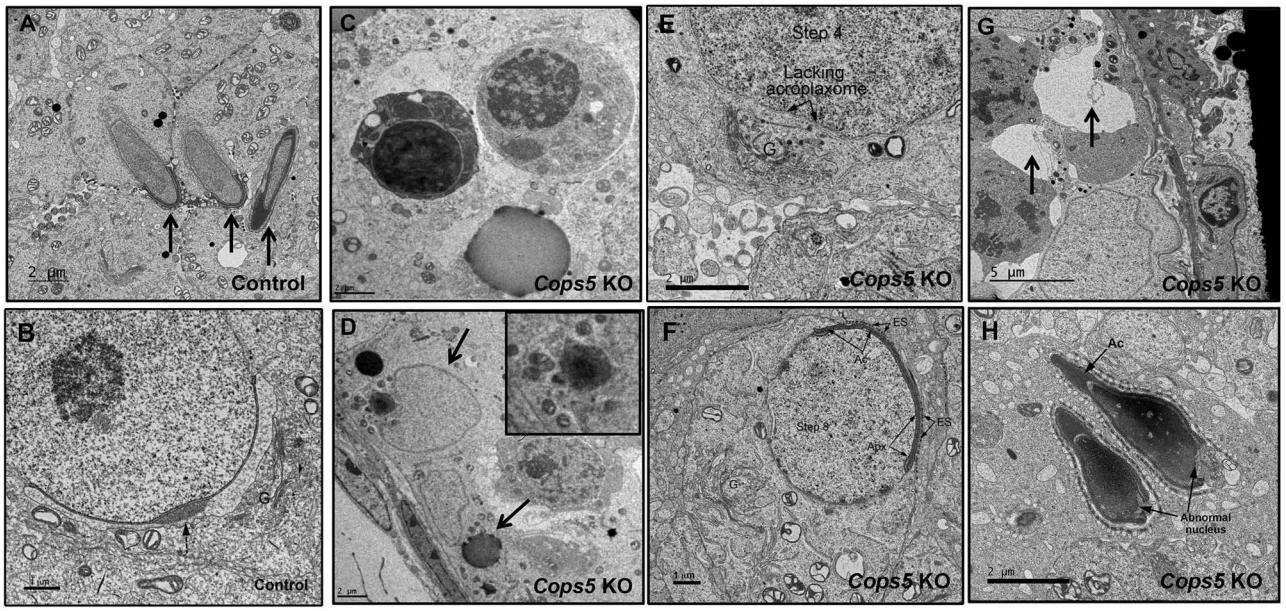

Figure 8. Ultra-structural changes in the seminiferous tubules of *Cops5* knockout mice. A. Normally developed elongating spermatids (arrows) in a control mouse. B. Normally developed round spermatid in a control mouse, showing a well-developed acrosome (arrow) and a prominent Golgi apparatus (G). C. Representative apoptotic germ cells in the seminiferous epithelium of the *Cops5* KO. D. Apoptotic cells are being engulfed by Sertoli cells. The upper arrow is pointing to a Sertoli cell nucleus. The black debris is the left-over material after digestion (lower arrow). E. Step 4 round spermatid showing failure of acrosome formation in the flattened area under the Golgi apparatus (G), where the acroplaxome is also missing. F. A round spermatid in the *Cops5* KO that has a thin acrosome but formed an abnormal ectoplasmic specialization (ES) with the Sertoli cell. G. The arrows point to vacuoles, presumably the space left remaining after apoptotic cells have been phagocyted by Sertoli cells. H. Two elongated spermatids that formed what appear to be normal acrosomes, but show abnormal nuclear structures.

ubiquitination in germ cells. In the absence of COPS5, FANK1 ubiquitination level was changed, and this could have induced apoptosis. In addition to FANK1, other proteins including IFT20 might also require COPS5 to be ubiquitinated. Thus, identification of the proteins ubiquitinated globally in male germ cells will provide a greater understanding of the mechanism of COPS5 in the regulation of spermatogenesis.

Although infertile, the conditional *Cops5* knockout testis still generated a few elongated spermatids and a few epididymal sperm. However, these cells were abnormal. It would be interesting to examine function of these sperm by IVF and ICSI in the future so that multiple aspects of the mutant sperm can be characterized, and mechanisms of COPS5 in male fertility can be further investigated. Due to impaired motility, we do not expect IVF will succeed. It would be difficult to predict outcome of ICSI because this will also be dependent on many aspects of sperm DNA.

Acknowledgments

We thank Dr. Gregory J Pazour for providing IFT20/Flag plasmid and anti-IFT20 antibody and Dr. Richard Oko at Queens University for providing the anti-SPACA1 antibody for our study. Dr. Scott C. Henderson and Judy C. Williamson for their assistance with using the electronic microscopy in Microscopy Core Facility of Virginia Commonwealth University, and Dr. Alicia Withrow for using the electronic microscopy in Center for Advanced Microscopy of Michigan State University.

Conflict of interest

There is no conflict of interest that could be perceived as prejudicing the impartiality of the research reported.

References

1. Claret FX, Hibi M, Dhut S, Toda T, Karin M. A new group of conserved coactivators that increase the specificity of AP-1 transcription factors. *Nature* 1996; **383**:453–457.
2. Cope GA, Suh GS, Aravind L, Schwarz SE, Zipursky SL, Koonin EV, Deshaies RJ. Role of predicted metalloprotease motif of Jab1/Csn5 in cleavage of Nedd8 from Cul1. *Science* 2002; **298**:608–611.
3. Bech-Otschir D, Kraft R, Huang X, Henklein P, Kapelari B, Pollmann C, Dubiel W. COP9 signalosome-specific phosphorylation targets p53 to degradation by the ubiquitin system. *EMBO J* 2001; **20**:1630–1639.
4. Wei N, Deng XW. COP9: a new genetic locus involved in light-regulated development and gene expression in arabidopsis. *Plant Cell* 1992; **4**:1507–1518.
5. Wei N, Tsuge T, Serino G, Dohmae N, Takio K, Matsui M, Deng XW. The COP9 complex is conserved between plants and mammals and is related to the 26S proteasome regulatory complex. *Curr Biol* 1998; **8**:919–922.
6. Dubiel D, Rockel B, Naumann M, Dubiel W. Diversity of COP9 signalosome structures and functional consequences. *FEBS Lett* 2015; **589**:2507–2513.
7. Cavadini S, Fischer ES, Bunker RD, Potenza A, Lingaraju GM, Goldie KN, Mohamed WI, Faty M, Petzold G, Beckwith RE, Tichkule RB, Hassiepen U et al. Cullin-RING ubiquitin E3 ligase regulation by the COP9 signalosome. *Nature* 2016; **531**:598–603.
8. Bornstein G, Ganoth D, Hershko A. Regulation of neddylation and deneddylation of cullin1 in SCFSkp2 ubiquitin ligase by F-box protein and substrate. *Proc Natl Acad Sci U S A* 2006; **103**:11515–11520.
9. Tomoda K, Kubota Y, Kato J. Degradation of the cyclin-dependent-kinase inhibitor p27Kip1 is instigated by Jab1. *Nature* 1999; **398**:160–165.
10. Kleemann R, Hausser A, Geiger G, Mischke R, Burger-Kentischer A, Flieger O, Johannes FJ, Roger T, Calandra T, Kapurniotu A, Grell M, Finkelmeier D et al. Intracellular action of the cytokine MIF to modulate AP-1 activity and the cell cycle through Jab1. *Nature* 2000; **408**:211–216.

11. Hallstrom TC, Nevins JR. Jab1 is a specificity factor for E2F1-induced apoptosis. *Genes Dev* 2006; **20**:613–623.
12. Liu X, Pan Z, Zhang L, Sun Q, Wan J, Tian C, Xing G, Yang J, Liu X, Jiang J, He F. JAB1 accelerates mitochondrial apoptosis by interaction with proapoptotic BclGs. *Cell Signal* 2008; **20**:230–240.
13. Jumpertz S, Hennes T, Asare Y, Schutz AK, Bernhagen J. CSN5/JAB1 suppresses the WNT inhibitor DKK1 in colorectal cancer cells. *Cell Signal* 2017; **34**:38–46.
14. Lue H, Kapurniotu A, Fingerle-Rowson G, Roger T, Leng L, Thiele M, Calandra T, Bucala R, Bernhagen J. Rapid and transient activation of the ERK MAPK signalling pathway by macrophage migration inhibitory factor (MIF) and dependence on JAB1/CSN5 and Src kinase activity. *Cell Signal* 2006; **18**:688–703.
15. Lee MH, Zhao R, Phan L, Yeung SC. Roles of COP9 signalosome in cancer. *Cell Cycle* 2011; **10**:3057–3066.
16. Adler AS, Littlepage LE, Lin M, Kawahara TL, Wong DJ, Werb Z, Chang HY. CSN5 isopeptidase activity links COP9 signalosome activation to breast cancer progression. *Cancer Res* 2008; **68**: 506–515.
17. Chamovitz DA, Segal D. JAB1/CSN5 and the COP9 signalosome. A complex situation. *EMBO Rep* 2001; **2**:96–101.
18. Oron E, Mannervik M, Rencus S, Harari-Steinberg O, Neuman-Silberberg S, Segal D, Chamovitz DA. COP9 signalosome subunits 4 and 5 regulate multiple pleiotropic pathways in *Drosophila melanogaster*. *Development* 2002; **129**:4399–4409.
19. Li P, Xie L, Gu Y, Li J, Xie J. Roles of multifunctional COP9 signalosome complex in cell fate and implications for drug discovery. *J Cell Physiol* 2017; **232**:1246–1253.
20. Ambroggio XI, Rees DC, Deshaies RJ. JAMM: a metalloprotease-like zinc site in the proteasome and signalosome. *PLoS Biol* 2004; **2**: E2.
21. Wei N, Deng XW. The COP9 signalosome. *Annu Rev Cell Dev Biol* 2003; **19**:261–286.
22. Lingaraju GM, Bunker RD, Cavadini S, Hess D, Hassiepen U, Renatus M, Fischer ES, Thoma NH. Crystal structure of the human COP9 signalosome. *Nature* 2014; **512**:161–165.
23. Schwechheimer C, Deng XW. COP9 signalosome revisited: a novel mediator of protein degradation. *Trends Cell Biol* 2001; **11**:420–426.
24. Wolf DA, Zhou C, Wee S. The COP9 signalosome: an assembly and maintenance platform for cullin ubiquitin ligases? *Nat Cell Biol* 2003; **5**:1029–1033.
25. Duda DM, Borg LA, Scott DC, Hunt HW, Hammel M, Schulman BA. Structural insights into NEDD8 activation of cullin-RING ligases: conformational control of conjugation. *Cell* 2008; **134**: 995–1006.
26. Shackleford TJ, Claret FX. JAB1/CSN5: a new player in cell cycle control and cancer. *Cell Div* 2010; **5**:26.
27. Maytal-Kivity V, Piran R, Pick E, Hofmann K, Glickman MH. COP9 signalosome components play a role in the mating pheromone response of S. cerevisiae. *EMBO Rep* 2002; **3**:1215–1221.
28. Liu G, Claret FX, Zhou F, Pan Y. Jab1/COPS5 as a novel biomarker for diagnosis, prognosis, therapy prediction and therapeutic tools for human cancer. *Front Pharmacol* 2018; **9**:135.
29. Bhansali M, Shemshedini L. COP9 subunits 4 and 5 target soluble guanylyl cyclase alpha1 and p53 in prostate cancer cells. *Mol Endocrinol* 2014; **28**:834–845.
30. Kouvaraki MA, Rassidakis GZ, Tian L, Kumar R, Kittas C, Claret FX. Jun activation domain-binding protein 1 expression in breast cancer inversely correlates with the cell cycle inhibitor p27(Kip1). *Cancer Res* 2003; **63**:2977–2981.
31. Osoegawa A, Yoshino I, Kometani T, Yamaguchi M, Kameyama T, Yohena T, Maehara Y. Overexpression of Jun activation domain-binding protein 1 in nonsmall cell lung cancer and its significance in p27 expression and clinical features. *Cancer* 2006; **107**:154–161.
32. Kim BC, Lee HJ, Park SH, Lee SR, Karpova TS, McNally JG, Felici A, Lee DK, Kim SJ. Jab1/CSN5, a component of the COP9 signalosome, regulates transforming growth factor beta signaling by binding to Smad7 and promoting its degradation. *Mol Cell Biol* 2004; **24**: 2251–2262.
33. Schutz AK, Hennes T, Jumpertz S, Fuchs S, Bernhagen J. Role of CSN5/JAB1 in Wnt/beta-catenin activation in colorectal cancer cells. *FEBS Lett* 2012; **586**:1645–1651.
34. Orel L, Neumeier H, Hochrainer K, Binder BR, Schmid JA. Crosstalk between the NF-kappaB activating IKK-complex and the CSN signalosome. *J Cell Mol Med* 2010; **14**:1555–1568.
35. Zhou F, Pan Y, Wei Y, Zhang R, Bai G, Shen Q, Meng S, Le XF, Andreeff M, Claret FX. Jab1/Csn5-thioredoxin signaling in relapsed acute monocytic leukemia under oxidative stress. *Clin Cancer Res* 2017; **23**:4450–4461.
36. Bemis L, Chan DA, Finkielstein CV, Qi L, Sutphin PD, Chen X, Stenmark K, Giaccia AJ, Zundel W. Distinct aerobic and hypoxic mechanisms of HIF-alpha regulation by CSN5. *Genes Dev* 2004; **18**:739–744.
37. Yoshida A, Yoneda-Kato N, Kato JY. CSN5 specifically interacts with CDK2 and controls senescence in a cytoplasmic cyclin E-mediated manner. *Sci Rep* 2013; **3**:1054.
38. Stobdan T, Akbari A, Azad P, Zhou D, Poulsen O, Appenzeller O, Gonzales GF, Telenti A, Wong EHM, Saini S, Kirkness EF, Venter JC et al. New insights into the genetic basis of Monge's disease and adaptation to high-altitude. *Mol Biol Evol* 2017; **34**:3154–3168.
39. Malhotra AG, Jha M, Singh S, Pandey KM. Construction of a comprehensive protein-protein interaction map for Vitiligo disease to identify key regulatory elements: a systemic approach. *Interdiscip Sci* 2018; **10**:500–514.
40. Schwarz A, Bonaterra GA, Schwarzbach H, Kinscherf R. Oxidized LDL-induced JAB1 influences NF-kappaB independent inflammatory signaling in human macrophages during foam cell formation. *J Biomed Sci* 2017; **24**:12.
41. Omede A, Zi M, Prehar S, Maqsood A, Stafford N, Mamas M, Cartwright E, Oceandy D. The oxoglutarate receptor 1 (OXGR1) modulates pressure overload-induced cardiac hypertrophy in mice. *Biochem Biophys Res Commun* 2016; **479**:708–714.
42. Wang R, Wang H, Carrera I, Xu S, Lakshmana MK. COPS5 protein overexpression increases amyloid plaque burden, decreases spinophilin-immunoreactive puncta, and exacerbates learning and memory deficits in the mouse brain. *J Biol Chem* 2015; **290**:9299–9309.
43. Cayli S, Eyibilen A, Gurbuzler L, Koc S, Atay GA, Ekici A, Aladag I. Jab1 expression is associated with TGF-beta1 signaling in chronic rhinosinusitis and nasal polyposis. *Acta Histochem* 2012; **114**:12–17.
44. Tanguy G, Drevillon L, Arous N, Hasnain A, Hinzpeter A, Fritsch J, Goossens M, Fanen P. CSN5 binds to misfolded CFTR and promotes its degradation. *Biochim Biophys Acta* 1783; **2008**:1189–1199.
45. Haag J, Aigner T. Jun activation domain-binding protein 1 binds Smad5 and inhibits bone morphogenetic protein signaling. *Arthritis Rheum* 2006; **54**:3878–3884.
46. Kinoshita SM, Krutzik PO, Nolan GP. COP9 signalosome component JAB1/CSN5 is necessary for T cell signaling through LFA-1 and HIV-1 replication. *PLoS One* 2012; **7**:e41725.
47. Tomoda K, Yoneda-Kato N, Fukumoto A, Yamanaka S, Kato JY. Multiple functions of Jab1 are required for early embryonic development and growth potential in mice. *J Biol Chem* 2004; **279**:43013–43018.
48. Panattoni M, Sanvito F, Basso V, Doglioni C, Casorati G, Montini E, Bender JR, Mondino A, Pardi R. Targeted inactivation of the COP9 signalosome impairs multiple stages of T cell development. *J Exp Med* 2008; **205**:465–477.
49. Bashur LA, Chen D, Chen Z, Liang B, Pardi R, Murakami S, Zhou G. Loss of jab1 in osteochondral progenitor cells severely impairs embryonic limb development in mice. *J Cell Physiol* 2014; **229**:1607–1617.
50. Cayli S, Demirturk F, Ocakli S, Aytan H, Caliskan AC, Cimsir H. Altered expression of COP9 signalosome proteins in preeclampsia. *Gynecol Endocrinol* 2012; **28**:488–491.
51. Kim E, Yoon SJ, Kim EY, Kim Y, Lee HS, Kim KH, Lee KA. Function of COP9 signalosome in regulation of mouse oocytes meiosis by regulating MPF activity and securing degradation. *PLoS One* 2011; **6**: e25870.

52. Khan DR, Landry DA, Fournier E, Vigneault C, Blondin P, Sirard MA. Transcriptome meta-analysis of three follicular compartments and its correlation with ovarian follicle maturity and oocyte developmental competence in cows. *Physiol Genomics* 2016; **48**:633–643.
53. Zheng Z, Zheng H, Yan W. Fank1 is a testis-specific gene encoding a nuclear protein exclusively expressed during the transition from the meiotic to the haploid phase of spermatogenesis. *Gene Expression Patterns* 2007; **7**:777–783.
54. Wang H, Song W, Hu T, Zhang N, Miao S, Zong S, Wang L. Fank1 interacts with Jab1 and regulates cell apoptosis via the AP-1 pathway. *Cell Mol Life Sci* 2011; **68**:2129–2139.
55. Dong WW, Huang HL, Yang W, Liu J, Yu Y, Zhou SL, Wang W, Lv XC, Li ZY, Zhang MY, Zheng ZH, Yan W. Testis-specific Fank1 gene in knockdown mice produces oligospermia via apoptosis. *Asian J Androl* 2014; **16**:124–130.
56. Zhang Z, Li W, Zhang Y, Zhang L, Teves ME, Liu H, Strauss JF 3rd, Pazour GJ, Foster JA, Hess RA, Zhang Z. Intraflagellar transport protein IFT20 is essential for male fertility and spermiogenesis in mice. *Mol Biol Cell* 2016.
57. Liu H, Li W, Zhang Y, Zhang Z, Shang X, Zhang L, Zhang S, Li Y, Somoza AV, Delpi B, Gerton GL, Foster JA et al. IFT25, an intraflagellar transporter protein dispensable for ciliogenesis in somatic cells, is essential for sperm flagella formation. *Biol Reprod* 2017; **96**: 993–1006.
58. Zhang Y, Liu H, Li W, Zhang Z, Shang X, Zhang D, Li Y, Zhang S, Liu J, Hess RA, Pazour GJ, Zhang Z. Intraflagellar transporter protein (IFT27), an IFT25 binding partner, is essential for male fertility and spermiogenesis in mice. *Dev Biol* 2017; **432**:125–139.
59. Zhang Y, Liu H, Li W, Zhang Z, Zhang S, Teves ME, Stevens C, Foster JA, Campbell GE, Windle JJ, Hess RA, Pazour GJ et al. Intraflagellar transporter protein 140 (IFT140), a component of IFT-a complex, is essential for male fertility and spermiogenesis in mice. *Cytoskeleton (Hoboken)* 2018; **75**:70–84.
60. Mao J, Pennington KA, Talton OO, Schulz LC, Sutovsky M, Lin Y, Sutovsky P. In utero and postnatal exposure to high fat, high sucrose diet suppressed testis apoptosis and reduced sperm count. *Sci Rep* 2018; **8**:7622.
61. Zhang Z, Shen X, Gude DR, Wilkinson BM, Justice MJ, Flickinger CJ, Herr JC, Eddy EM, Strauss JF 3rd. MEIG1 is essential for spermiogenesis in mice. *Proc Natl Acad Sci U S A* 2009; **106**: 17055–17060.
62. Hao Z, Wolkowicz MJ, Shetty J, Klotz K, Bolling L, Sen B, Westbrook VA, Coonrod S, Flickinger CJ, Herr JC. SAMP32, a testis-specific, isoantigenic sperm acrosomal membrane-associated protein. *Biol Reprod* 2002; **66**:735–744.
63. Rosenbaum JL, Witman GB. Intraflagellar transport. *Nat Rev Mol Cell Biol* 2002; **3**:813–825.
64. Reiter JF, Leroux MR. Genes and molecular pathways underpinning ciliopathies. *Nat Rev Mol Cell Biol* 2017; **18**:533–547.
65. Kierszenbaum AL, Tres LL. The acrosome-acroplaxome-manchette complex and the shaping of the spermatid head. *Arch Histol Cytol* 2004; **67**:271–284.
66. Follit JA, Tuft RA, Fogarty KE, Pazour GJ. The intraflagellar transport protein IFT20 is associated with the Golgi complex and is required for cilia assembly. *Mol Biol Cell* 2006; **17**:3781–3792.
67. Marshall WF. Basal bodies platforms for building cilia. *Curr Top Dev Biol* 2008; **85**:1–22.
68. Ng KK, Donat R, Chan L, Lalak A, Di Pierro I, Handelsman DJ. Sperm output of older men. *Hum Reprod* 2004; **19**:1811–1815.
69. Huckins C, Oakberg EF. Morphological and quantitative analysis of spermatogonia in mouse testes using whole mounted seminiferous tubules, I. the normal testes. *Anat Rec* 1978; **192**: 519–528.
70. Almeida C, Correia S, Rocha E, Alves A, Ferraz L, Silva J, Sousa M, Barros A. Caspase signalling pathways in human spermatogenesis. *J Assist Reprod Genet* 2013; **30**:487–495.
71. Russell LD, Warren J, Debeljuk L, Richardson LL, Mahar PL, Waymire KG, Amy SP, Ross AJ, MacGregor GR. Spermatogenesis in Bclw-deficient mice. *Biol Reprod* 2001; **65**:318–332.
72. Jahnukainen K, Chrysis D, Hou M, Parvinen M, Eksborg S, Soder O. Increased apoptosis occurring during the first wave of spermatogenesis is stage-specific and primarily affects midpachytene spermatocytes in the rat testis. *Biol Reprod* 2004; **70**:290–296.
73. Shaha C, Tripathi R, Mishra DP. Male germ cell apoptosis: regulation and biology. *Philos Trans R Soc Lond B Biol Sci* 2010; **365**:1501–1515.
74. Yan W, Kero J, Huhtaniemi I, Toppari J. Stem cell factor functions as a survival factor for mature Leydig cells and a growth factor for precursor Leydig cells after ethylene dimethane sulfonate treatment: implication of a role of the stem cell factor/c-kit system in Leydig cell development. *Dev Biol* 2000; **227**:169–182.
75. Yan W, Suominen J, Samson M, Jegou B, Toppari J. Involvement of Bcl-2 family proteins in germ cell apoptosis during testicular development in the rat and pro-survival effect of stem cell factor on germ cells in vitro. *Mol Cell Endocrinol* 2000; **165**:115–129.
76. Yan W, Samson M, Jegou B, Toppari J. Bcl-w forms complexes with Bax and Bak, and elevated ratios of Bax/Bcl-w and Bak/Bcl-w correspond to spermatogonial and spermatocyte apoptosis in the testis. *Mol Endocrinol* 2000; **14**:682–699.
77. Doyle TJ, Braun KW, McLean DJ, Wright RW, Griswold MD, Kim KH. Potential functions of retinoic acid receptor a in sertoli cells and germ cells during spermatogenesis. *Ann N Y Acad Sci* 2007; **1120**: 114–130.
78. Toppari J, Suominenf JS, Yan W. The role of retinoblastoma protein family in the control of germ cell proliferation, differentiation and survival. *APMIS* 2003; **111**:245–251.
79. Fan YS, Hu YJ, Yang WX. TGF-beta superfamily: how does it regulate testis development. *Mol Biol Rep* 2012; **39**:4727–4741.
80. Ren X, Song W, Liu W, Guan X, Miao F, Miao S, Wang L. Rhomboid domain containing 1 inhibits cell apoptosis by upregulating AP-1 activity and its downstream target Bcl-3. *FEBS Lett* 2013; **587**:1793–1798.
81. Nie D, Liu Y, Xiang Y. Overexpression a novel zebra fish spermatogenesis-associated gene 17 (SPATA17) induces apoptosis in GC-1 cells. *Mol Biol Rep* 2011; **38**:3945–3952.
82. Liu ML, Cheng YM, Jia MC. LM23 is essential for spermatogenesis in *Rattus norvegicus*. *Front Biosci (Elite Ed)* 2010; **2**:187–194.
83. Finley D, Chau V. Ubiquitination. *Annu Rev Cell Biol* 1991; **7**:25–69.
84. Chen HY, Sun JM, Zhang Y, Davie JR, Meistrich ML. Ubiquitination of histone H3 in elongating spermatids of rat testes. *J Biol Chem* 1998; **273**:13165–13169.
85. Sidjanin DJ, Park AK, Ronchetti A, Martins J, Jackson WT. TBC1D20 mediates autophagy as a key regulator of autophagosome maturation. *Autophagy* 2016; **12**:1759–1775.
86. Foot N, Henshall T, Kumar S. Ubiquitination and the regulation of membrane proteins. *Physiol Rev* 2017; **97**:253–281.
87. Fritsch J, Zingler P, Sarchen V, Heck AL, Schutze S. Role of ubiquitination and proteolysis in the regulation of pro- and anti-apoptotic TNF-R1 signaling. *Biochim Biophys Acta* 1864; **2017**:2138–2146.
88. Ma W, Zhang X, Li M, Ma X, Huang B, Chen H, Chen D. Proapoptotic RYBP interacts with FANK1 and induces tumor cell apoptosis through the AP-1 signaling pathway. *Cell Signal* 2016; **28**: 779–787.